Journal of Computational Physics 229 (2010) 527–540

Contents lists available at ScienceDirect

Journal of Computational Physics

journal homepage: www.elsevier.com/locate/jcp

Interface curvature via volume fractions, heights, and mean values on nonuniform rectangular grids

Marianne M. Francois [a,*], Blair K. Swartz [b]

[a] Computational Physics and Methods (CCS-2), Los Alamos National Laboratory, United States
[b] Applied Mathematics and Plasma Physics (T-5), Los Alamos National Laboratory, United States

ARTICLE INFO

Article history:
Received 12 May 2009
Received in revised form 7 October 2009
Accepted 13 October 2009
Available online 21 October 2009

Keywords:
Volume-of-fluid
Curvature
Height function
Mean value
Nonuniform grids
Numerical differentiation

ABSTRACT

Estimating the local curvature of an interface involves the local determination of normals to the interface, and the rates that they turn along the interface. This is challenging in volume-of-fluid type methods since the interface between materials is specified by the relative amount it cuts off from the computational cells that it crosses (also referred to as volume fraction data) rather than by a discrete set of points lying on the interface itself. In this work, we generalize the height function method to nonuniform rectangular grids. We demonstrate analytically and numerically that—using three successive (adjacent) integral mean values (or "column" heights)—interface curvature can be estimated to second-order accuracy, the first derivative (interface normal) to third-order accuracy, and the curve location to fourth-order accuracy—each at its own special points. We also show that there are special points where the curvature can be estimated to fourth-order accuracy when using five successive mean values instead.

Underlying all this is a result about the accuracy of the jth-derivative of the kth-degree polynomial that interpolates a function F at $k+1$ stencil points placed irregularly in an interval of width h. Namely, for all smooth enough functions F and for k fixed and h getting small, there are $k+1-j$ special points in the interval at which the error in the jth derivative is of order $O(h^{k+2-j})$. (This is one order higher than the usual $O(h^{k+1-j})$ error holding over the whole interval for that derivative.) The special points in the interval are the $k+1-j$ (real) zeroes of certain F-independent polynomials, of degree $k+1-j$, with coefficients depending on the interval's stencil points.

In our case, let $F(x)$ be an indefinite integral of the unknown interfacial curve $f(x)$. Then $F(x_i)$ at $k+1$ successive stencil points x_i is calculated using cumulative sums of the k successive integral mean values of f, weighted by the successive interval sizes. The $k+1$ points $(x_i, F(x_i))$ are now interpolated by a kth degree polynomial $(PF)(x)$. It's first derivative $(PF)^{(1)}$ approximates the unknown curve f; while $(PF)^{(2)}$ and $(PF)^{(3)}$, respectively, approximate $f^{(1)}$ and $f^{(2)}$. Thus, the results above using three successive mean values correspond to $k=3$ and $j=3,2,1$. The curvature result using five successive mean values correspond to $k=5$ and $j=3$. For this last case, since the curvature $\kappa = f^{(2)}/(1+(f^{(1)})^2)^{3/2}$, we use the facts that $f^{(1)} = F^{(2)} = (PF)^{(2)} + O(h^4)$ on the whole stencil interval, not just at the three special points having $O(h^4)$ accuracy for $f^{(2)}$.

* Corresponding author. Address: MS B296, P.O. Box 1663, Los Alamos National Laboratory, Los Alamos, NM 87545, United States.
E-mail addresses: mmfran@lanl.gov (M.M. Francois), bks@lanl.gov (B.K. Swartz).

0021-9991/$ - see front matter
doi:10.1016/j.jcp.2009.10.022

1. Introduction

In volume-of-fluid methods the interface between regions is specified by the relative amount the interface cuts off from the computational cells that it crosses, rather than by a discrete set of points lying on the interface itself. But estimating the local curvature of an interface involves the local determination of normals to the interface, and the rates that they turn along the interface. This might seem problematic using such locally smeared information as fractional amounts cut off from interfacial cells. Nevertheless, for a two-dimensional uniform grid of square mesh cells with corners $(x_i, y_j)_{i=1}^{m}{}_{j=1}^{n}$, one may first choose a local vertical direction (say, the increasing y direction) from the four possibilities available (x or y—increasing or decreasing). Then, one may define a local height for the interface in each of three neighboring "vertical" columns of cells—columns associated with, say,

$$x_i \leqslant x \leqslant x_{i+1}, \quad x_{i+1} \leqslant x \leqslant x_{i+2}, \quad \text{and} \quad x_{i+2} \leqslant x \leqslant x_{i+3}$$

by summing all partial areas in a column below the interface but above a horizontal floor common to the three intervals. Dividing by the column width, this succeeds in defining a local piecewise-constant interfacial "height function" for the interface:

$$H(x) = H_{i+1/2}, \quad x_i \leqslant x < x_{i+1}, \quad i = 2, \ldots, N-1. \tag{1}$$

The two derivatives in the relevant expression for the local curvature of the interface, namely,

$$\kappa := \frac{d^2y/dx^2}{[1 + (dy/dx)^2]^{3/2}} \tag{2}$$

are now estimated by applying centered difference formulas to the related discrete function

$$(x_{m+1/2}, H_{m+1/2}), \quad x_{m+1/2} := (x_m + x_{m+1})/2, \quad m = i, i+1, i+2. \tag{3}$$

The estimate is demonstrably second-order accurate at the mid-point of the intersection of the interface with the middle column, see e.g. Cummins et al. [3].

The "height function" method [15,7] has mainly been used on uniform rectangular meshes. For such grids, it has been demonstrated to yield second-order accuracy using three successive heights $H_{i+1/2}$ (or columns) for both interface curvatures [13,10,3,5] and interface normals [4]. The method has also been extended to compute fourth-order accurate curvature using five successive heights $H_{i+1/2}$ (or columns) [14]. Recent studies on the height function method have focused on improving the estimation of the height function itself by choosing the best local rectangular set of mesh squares [16,8,1,12]. The focus of this note is not on the choice of the optimum set of mesh squares for estimating the height function.

Instead, this note focuses on showing, both analytically and numerically, that given (integral) mean values (or column heights) associated with three adjacent columns of a nonuniform grid, we can compute second-order accurate curvature associated with the average location of the four successive grid points. For the case of a uniform grid this four-point average location is the location of the mid-point of the middle interval. We also find locations in each stencil interval where third-order accurate approximate first derivatives, and fourth-order accurate points on the curve, can be (and are) calculated. Finally, we extend a recent fourth-order accurate curvature result of Sussman and Ohta [14], based on five adjacent uniform columns, to nonuniform rectangular grids.

2. Nonuniform rectangular grids

This note extends the height function result to nonuniform "tensor product" grids; that is to say, to grids of mesh points

$$(x_i, y_j)_{i=1}^{m}{}_{j=1}^{n}, \quad x_0 < x_1 < \cdots < x_m, \quad y_0 < y_1 < \cdots < y_n$$

that are not necessarily uniformly spaced (see Fig. 1). The result is more clearly stated and analyzed in terms of the single-valued function $(x, f(x))$, presumed to describe the interface locally, along with f's integral mean values

$$\bar{f}_{i+1/2} := \frac{\int_{x_i}^{x_{i+1}} f(t)\,dt}{(x_{i+1} - x_i)}. \tag{4}$$

The sequence $\bar{f}$ is the present analog of the "height function", and is presumed to be known data.

We now suppose that the (unknown) interfacial curve $(x, f(x))$ crosses four successive vertical mesh lines $x = x_i, \ldots, x = x_{i+3}$. Let now $F(x)$ be an indefinite integral of the interfacial curve function $f(x)$. Then

$$\left(\frac{dF}{dx}\right)(x) = f(x), \quad \text{and} \quad \left(\frac{\Delta F}{\Delta x}\right)_{i+1/2} := \frac{[F(x_{i+1}) - F(x_i)]}{(x_{i+1} - x_i)} = \bar{f}_{i+1/2} \tag{5}$$

are the (unknown) derivative and the (known) first difference quotient of F, respectively. More important for curvature estimates of the curve are the (unknown) second and third derivatives of F and its (known) second and third difference quotients:

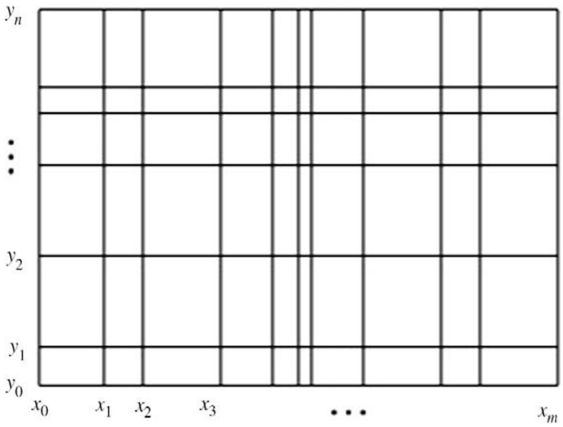

Fig. 1. Illustration of nonuniform "tensor product" grid.

$$\frac{d^2F}{dx^2} = \frac{df}{dx} \quad \text{and} \quad \left(\frac{\Delta^2 F}{\Delta x^2}\right)_{i+1} = \frac{(\bar{f}_{i+3/2} - \bar{f}_{i+1/2})}{[(x_{i+2} - x_i)/2]} \tag{6}$$

together with

$$\frac{d^3F}{dx^3} = \frac{d^2f}{dx^2} \quad \text{and} \quad \left(\frac{\Delta^3 F}{\Delta x^3}\right)_{i+3/2} := \frac{\left(\left(\frac{\Delta^2 F}{\Delta x^2}\right)_{i+2} - \left(\frac{\Delta^2 F}{\Delta x^2}\right)_{i+1}\right)}{[(x_{i+3} - x_i)/3]}. \tag{7}$$

(Just as the second difference quotient is the value of the second derivative of the quadratic interpolant of three successive points $(x_k, F_k)_{k=i}^{i+2}$, the third difference quotient is the value of the third derivative of the cubic polynomial interpolating the four points $(x_k, F_k)_{k=i}^{i+3}$.)

Let the width of the stencil be called

$$h := x_{i+3} - x_i; \tag{8}$$

it is presumed to be getting small (so that adjacent mesh points are getting close together). It is a fact that, while the third difference quotient of F approximates the third derivative of F to within first-order $O(h)$ accuracy when one is within $O(h)$ of the interval $[x_i, x_{i+3}]$, it approximates it to within *second*-order $O(h^2)$ accuracy near one special point; namely, within $O(h^2)$ of the average location

$$\bar{x}^{(4)}_{i+3/2} := \frac{(x_i + \cdots + x_{i+3})}{4} \tag{9}$$

of the four points in the difference stencil. For details, see the Remark in the next section. $\bar{x}^{(4)}_{i+3/2}$ is informally called a "four-point average".

In summary so far: we have an $O(h^2)$ accurate estimate of $(d^2f/dx^2)(\bar{x}^{(4)}_{i+3/2})$ using as data three successive means $\bar{f}_{i+1/2}$ of f (namely, $\bar{f}_{i+1/2}, \bar{f}_{i+3/2}$, and $\bar{f}_{i+5/2}$), i.e., three successive column-sums of (area-weighted) area fractions under the curve. For the curvature κ at $\bar{x}^{(4)}_{i+3/2}$ we also need to estimate the value of $df/dx = d^2F/dx^2$ at $\bar{x}^{(4)}_{i+3/2}$. We require $O(h^2)$ accuracy, using these same three successive means $\bar{f}_{i+1/2}$.

Towards this end: from the Remark, but for the *three*-point stencil (x_i, x_{i+1}, x_{i+2}), the second difference quotient Eq. (6) is a second-order accurate estimate for d^2F/dx^2 at the three-point average location

$$\bar{x}^{(3)}_{i+1} := \frac{(x_i + x_{i+1} + x_{i+2})}{3} \tag{10}$$

of its three associated stencil points. So, we estimate the needed value of $df/dx = d^2F/dx^2$ (and, with it, the curvature $\kappa = \kappa(x)$ of f) at the required four-point average $x = \bar{x}^{(4)}_{i+3/2}$ by linearly interpolating the two points

$$\left(\bar{x}^{(3)}_{i+1}, \left(\frac{\Delta^2 F}{\Delta x^2}\right)_{i+1}\right) \quad \text{and} \quad \left(\bar{x}^{(3)}_{i+2}, \left(\frac{\Delta^2 F}{\Delta x^2}\right)_{i+2}\right) \tag{11}$$

to that intermediate point $x = \bar{x}^{(4)}_{i+3/2}$. Note that, indeed, $\bar{x}^{(3)}_{i+1} < \bar{x}^{(4)}_{i+3/2} < \bar{x}^{(3)}_{i+2}$. See, for example, Fig. 2.

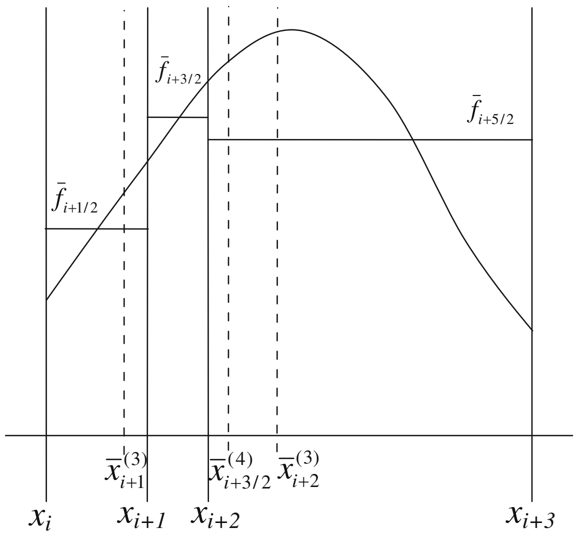

Fig. 2. Illustration of the position of four mesh points $x_i, x_{i+1}, x_{i+2}, x_{i+3}$, the three associated mean values $\bar{f}_{i+1/2}, \bar{f}_{i+3/2}, \bar{f}_{i+5/2}$, and the associated three-point average and four-point average locations $\bar{x}^{(3)}_{i+1}, \bar{x}^{(3)}_{i+2}, \bar{x}^{(4)}_{i+3/2}$ of the mesh points.

Finally: a continuous, $O(h^2)$ accurate function approximating the curvature $\kappa(x)$ along the curve is attained by:

(1) Defining a continuous piecewise-linear approximate curvature function by linear interpolation of the above approximate curvatures between successive four-point averages $(x_i + \cdots + x_{i+3})/4$ and $(x_{i+1} + \cdots + x_{i+4})/4$; or, alternatively,
(2a) Defining a continuous piecewise-linear approximate second-derivative f''_{approx} by linear interpolation of $\Delta^3 F/\Delta x^3$ between successive four-point averages $(x_i + \cdots + x_{i+3})/4$ and $(x_{i+1} + \cdots + x_{i+4})/4$, and
(2b) Defining a continuous piecewise-linear approximate first-derivative f'_{approx} by linear interpolation of $\Delta^2 F/\Delta x^2$ between successive three-point averages $(x_i + \cdots + x_{i+2})/3$ and $(x_{i+1} + \cdots + x_{i+3})/3$.
(2c) The resulting continuous approximate curvature function

$$\kappa_{\text{approx}} := \frac{f''_{\text{approx}}}{[1 + (f'_{\text{approx}})^2]^{3/2}} \tag{12}$$

has frequent jumps in its slope, since the three-point stencil averages and the four-point stencil averages interlace each other. A possible change in "floors" (Section 1) from one four-point stencil to the next would not affect continuity or accuracy, as the two quantities entering κ_{approx} are difference quotients of $\bar{f}$. But, a change in the "vertical" direction would be a different matter.

Note that approach (1) was taken in [5] in order to compute curvature at cell faces on a uniform square grid when the curvature was defined in two adjacent cells.

3. Where are the derivatives of polynomial interpolants especially accurate ?

For completeness we now sketch a proof of the Remark below; see Kreiss et al. [9, p. 38]. For application of the Remark to three-point curvature estimates for plane curves, see Mjolsness and Swartz [11, p. 219; and, esp., Section 4 there].

Suppose $k \geqslant 1$ is fixed. Given $k+1$ distinct stencil points $(t_i)_{i=0}^k$ in increasing order, the kth-order difference quotient $\Delta^k g/\Delta t^k$ of a function $g(t)$ is defined as the (constant value of the) kth derivative of the kth-degree polynomial that matches g at the stencil points. (Recall here that $\Delta^k g/\Delta t^k$ is $k!$ times the kth-order divided difference of g.) Close to the stencil, the number $\Delta^k g/\Delta t^k$ approximates $d^k g/dt^k$ to within first-order, $O(h)$, in the width h of the stencil if $d^{k+1}g/dt^{k+1}$ is continuous. But there is one point inside the stencil interval at which accuracy can be second-order, i.e., $O(h^2)$ as the stencil width h gets small:

Remark. The kth difference quotient is centered at the average location

$$\bar{t}^{(k+1)}_{k/2} := \frac{(t_0 + t_1 + \cdots + t_k)}{(k+1)} \tag{13}$$

of its stencil points $(t_i)_0^k$ in the following sense: Suppose $d^{k+2}g/dt^{k+2}$ is bounded, then

$$\frac{\Delta^k g}{\Delta t^k} = \left(\frac{d^k g}{dt^k}\right)\left(\bar{t}^{(k+1)}_{k/2}\right) + O(h^2). \tag{14}$$

To see this, let Pg be the kth degree polynomial interpolant of g at the $(t_i)_{i=0}^k$, and let

$$e(t) := (g - Pg)(t). \tag{15}$$

Suppose d^kg/dt^k is smooth (e.g. Lipschitz continuous). Rolle's Theorem says that there is a zero of de/dt strictly between any two zeroes of e; so the k zeroes of de/dt interlace the $k+1$ zeroes of e. Applying this successively to e, to $de/dt, \ldots$, and to $d^{k-1}e/dt^{k-1}$, there exists one zero z_k for d^ke/dt^k strictly between t_0 and t_k. Since d^ke/dt^k is smooth, d^ke/dt^k is $O(h)$ in size when one is within $O(h)$ of z_k; e.g. in the interval $[t_0, t_k]$. But we cannot locate z_k more precisely without assumption of additional smoothness.

Suppose, now, that $g(t) = t^{k+1}/(k+1)!$. Then the $(k+1)$th degree polynomial $e = g - Pg$, vanishing as it does at the $k+1$ stencil points, must be

$$e(t) = \frac{(t-t_0)(t-t_1)\ldots(t-t_k)}{(k+1)!} = \frac{\left[t^{k+1} - (t_0 + \cdots + t_k)t^k + \cdots + (-1)^{k+1}t_0t_1\ldots t_k\right]}{(k+1)!}. \tag{16}$$

(The coefficients here involve the elementary symmetric polynomials—or, functions—in the $k+1$ variables $t_0, \ldots, t_k$. See, for example, the web article "Symmetric Polynomial", esp. Eqs. (7)–(17) there, in Wolfram MathWorld [17].) Consequently,

$$\left(\frac{d^ke}{dt^k}\right)(t) = \left(\frac{d^k(g-Pg)}{dt^k}\right)(t)\left(= \left(\frac{d^kg}{dt^k}\right)(t) - \frac{\Delta^kg}{\Delta t^k}\right) = t - \frac{(t_0 + \cdots + t_k)}{(k+1)} \tag{17}$$

is linear, $O(h)$ on $[t_0, t_k]$, and vanishes when $t = \bar{t}_{k/2}^{(k+1)}$. The same is true if g is a polynomial of the form $q(t) + t^{k+1}/(k+1)!, q$ a polynomial of degree k. For then $Pq = q$, and thus Eqs. (16) and (17) still hold true.

Returning to more general g, and without loss of generality, assume the origin $t = 0$ is placed at the $(k+1)$-point average $\bar{t}_{k/2}^{(k+1)}$. We have supposed that $d^{k+1}g/dt^{k+1}$ is smooth, so that g has Maclaurin expansions

$$(M_mg)(t) = \sum_{j=0}^{m}(d^jg/dt^j)(0)t^j/j! \tag{18}$$

of all degrees $m \leqslant k+1$. Then,

$$g(t) = (M_{k+1}g + R_{k+1}g)(t) = (M_kg)(t) + \left(\frac{d^{k+1}g}{dt^{k+1}}\right)(0) \cdot \frac{t^{k+1}}{(k+1)!} + (R_{k+1}g)(t), \tag{19}$$

where $R_{k+1}g$, the remainder in Maclaurin approximation of degree $k+1$, has various exact representations. As $\Delta^k(\cdot)/\Delta t^k (= d^k(P(\cdot))/dt^k)$ acts linearly, we conclude from Eq. (19) that

$$\frac{\Delta^kg}{\Delta t^k} = \frac{d^k(PM_kg)}{dt^k} + \left(\frac{d^{k+1}g}{dt^{k+1}}\right)(0) \cdot \frac{d^k\left(P\left[\frac{t^{k+1}}{(k+1)!}\right]\right)}{dt^k} + \frac{d^k(PR_{k+1}g)}{dt^k}. \tag{20}$$

Since $P(M_k) = M_k$, the first term in the right side of Eq. (20) is $(d^kg/dt^k)(0)$. For the second term: take $t = 0$ in Eq. (17), so that we now have $\Delta^k[t^{k+1}/(k+1)!]/\Delta t^k = \bar{t}_{k/2}^{(k+1)}$ (=0 by assumption) . Thus,

$$\frac{\Delta^kg}{\Delta t^k} = \left(\frac{d^kg}{dt^k}\right)(0) + \left(\frac{d^{k+1}g}{dt^{k+1}}\right)(0) \cdot 0 + \frac{d^k(PR_{k+1}g)}{dt^k}. \tag{21}$$

Since $R_{k+1}g$ is $O(h^{k+2})$, the last term is $O(h^{k+2-k}) = O(h^2)$. So, the Remark is valid. (Indeed, because the degree k is fixed, the Remark is true as $h = t_k - t_0$ goes to zero independent of the relative locations of $t_1, \ldots, t_{k-1}$ in the mesh interval (t_0, t_k).)

Now, let us restate the Remark as follows:

Reworded remark. For a sufficiently smooth function $g(t)$, let $(Pg)(t)$ be its kth degree polynomial interpolant at the $k+1$ points $t_0 < t_1 < \cdots < t_k$. Then if $k \geqslant 1$, the constant function $d^k(Pg)/dt^k$ is a first-order accurate approximation to $d^k(g)/dt^k$ on the interval $[t_0, t_k]$; but it is second-order accurate at the point $t = \bar{t}_{k/2}^{(k+1)}$ Eq. (13).

To this we now add: If $k \geqslant 2$, the linear function $d^{k-1}(Pg)/dt^{k-1}$ is a second-order accurate approximation to $d^{k-1}g/dt^{k-1}$ on $[t_0, t_k]$; and there are two points in $[t_0, t_k]$, symmetric about $\bar{t}_{k/2}^{(k+1)}$, at which it is third-order accurate. Moreover, if $k \geqslant 3$, then the quadratic function $d^{k-2}(Pg)/dt^{k-2}$ is a third-order accurate approximation to $d^{k-2}g/dt^{k-2}$; and there are three points in $[t_0, t_k]$ at which it is fourth-order accurate.

More specifically, the two points where the linear approximate derivative is third-order accurate are the two roots of the quadratic $d^{k-1}e/dt^{k-1}$, where $e(t)$ (Eq. 16) is the relevant interpolation error. If the origin is placed at the mean value $\bar{t}_{k/2}^{(k+1)}$ (so that the mean value of the $k+1$ points $(t_i)_0^k$ is now 0), then these two points yielding special accuracy (assuming $\bar{t}_{k/2}^{(k+1)} = 0$) are

$$\tilde{t}_\pm := \pm\left[\left(t_0^2 + t_1^2 + \cdots + t_k^2\right)/(k(k+1))\right]^{1/2}. \tag{22}$$

In the same way, the three points yielding fourth-order accuracy when evaluating the quadratic approximate derivative $d^{k-2}(Pg)/dt^{k-2}$ are the three roots of the cubic $d^{k-2}e/dt^{k-2}$, with $e(t)$ Eq. (16) again the relevant interpolation error. We pointed out earlier, using successive applications of Rolle's theorem, that these three roots were real. Locating the $k+1$ stencil points relative to their average $\bar{t}_{k/2}^{(k+1)}$, so that, again, $\bar{t}_{k/2}^{(k+1)} = 0$, the cubic is in its "normal form" $t^3 + at + b$. Then, its three roots have well-known closed-form elementary expressions involving the coefficients

$$a = 6(t_0(t_1 + \cdots + t_k) + t_1(t_2 + \cdots + t_k) + \cdots + t_{k-1}t_k)/(k(k+1)) \tag{23}$$

and

$$b = -6(t_0t_1(t_2 + \cdots + t_k) + (t_0 + t_1)t_2(t_3 + \cdots + t_k) + \cdots + (t_0 + \cdots + t_{k-2})t_{k-1}t_k)/((k-1)k(k+1)) \tag{24}$$

of the cubic's linear and constant terms. Cf. Ref. [2, pp. 7–9]; or formulas (70)–(73) in the web article "Cubic Formula" in Wolfram MathWorld [17].

More generally, the $m \leqslant k$ points yielding $(m+1)$th-order accuracy—for the value of the $(m-1)$th degree approximate derivative $d^{k+1-m}(Pg)/dt^{k+1-m}$—are the m roots of the mth degree polynomial $d^{k+1-m}e/dt^{k+1-m}$, with $e(t)$ Eq. (16) again the relevant interpolation error. As before, the m roots are all real. But for $m \geqslant 5$, there are no explicit formulae for them.

Appendix A provides justification for the special accuracies associated with the special points.

These locations of one, two, and three points of special accuracy for the highest, next-to-highest, and next-to-next-to-highest derivative of the kth degree polynomial interpolant, respectively, seem to be an especially accurate fixation—as the width h of the stencil gets small (and with k fixed)—of the zeroes of the corresponding derivatives of the interpolation error—zeroes whose existence proved so useful in Cauchy's analysis via Rolle's Theorem of the error in polynomial interpolation (as mentioned in Ref. [6, pp. 79–80]).

Finally, it is tempting to think that one could start with (Cauchy's) error formula for polynomial interpolation $(P_k)g$ of degree k of a function g:

$$e_g(x) := (g - P_kg)(x) = \frac{g^{(k+1)}(\xi(x))}{(k+1)!}\prod_{i=0}^{k}(x - x_i) \tag{25}$$

and differentiate it once to find the error in the first derivative. The first resulting term is an $O(h^{k+1})$ term, and one can choose special values x such that the second term is zero. And so forth, for the errors in the second, third, etc. derivatives.

But, for our approach to curvature (where $k = 3$), we would need that the derivatives with respect to x of order up to three, of both $g^{(4)}(x)$ and $\xi(x)$ be bounded over the h-size interval of interest. But the properties of the derivatives of ξ, in particular, are rarely discussed. For example, $g^{(5)}$ could be only continuous. Why, then, should ξ have three derivatives on $[x_0, x_k]$? Indeed, why any derivatives? After all, according to [6, pp. 80–81], ξ, for each fixed x, is a solution $t = \xi$ of the equation

$$0 = g^{(4)}(t) - (k+1)!\frac{e_g(x)}{\prod_0^k(x - x_i)}. \tag{26}$$

Another problem is the additional smoothness requirement on g. In general, $g^{(4)}$ is only continuous; in our proof (Appendix A) its derivative is also continuous. But, we do not need seven derivatives for g.

4. Numerical results

In this section, we demonstrate numerically that our curvature approximation is second-order accurate, our first derivative approximation is third-order accurate, and our function approximation is fourth-order accurate, each at their respective special points.

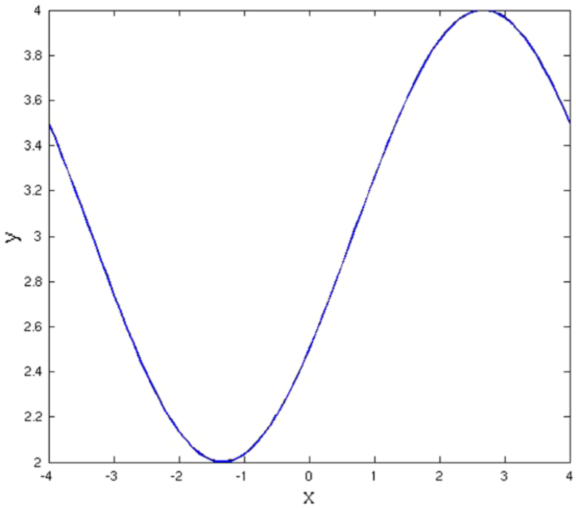

Fig. 3. Plot of the cosine function for the present numerical test cases.

For our numerical test cases, we consider the following cosine function:

$$f(x) = A - \cos\left(\frac{2\pi x}{L} + \frac{\pi}{3}\right), \quad (27)$$

with $A = 3$ and $L = 8$. This function is close to the one in Cummins et al. [3] but it has a phase shift of $\pi/3$ to avoid any possible symmetry with respect to our mesh stencils. The function is plotted in Fig. 3.

We consider four test cases of a stencil of four mesh points x_1, x_2, x_3, x_4. Each case distributes the points differently within the stencil but all have same mean $\bar{x}^{(4)}_{5/2} = 0$. Each test case is defined by its initial stencil width h (Eq. 8) and its successive mesh ratios R_1 and R_2,

$$R_1 = \frac{x_2 - x_1}{x_3 - x_2} \quad \text{and} \quad R_2 = \frac{x_3 - x_2}{x_4 - x_3}. \quad (28)$$

Specifically, these cases are:

(1) $h = 1.5,\ R_1 = R_2 = 1$ a uniform mesh,
(2) $h = 1.5,\ R_1 = R_2 = 0.9$ a nonuniform expanding mesh,
(3) $h = 1.5,\ R_1 = 0.1,\ R_2 = 10$ a nonuniform mesh symmetric with respect to the mean value and
(4) $h = 1.5,\ R_1 = 0.3,\ R_2 = 0.7$ a nonuniform mesh.

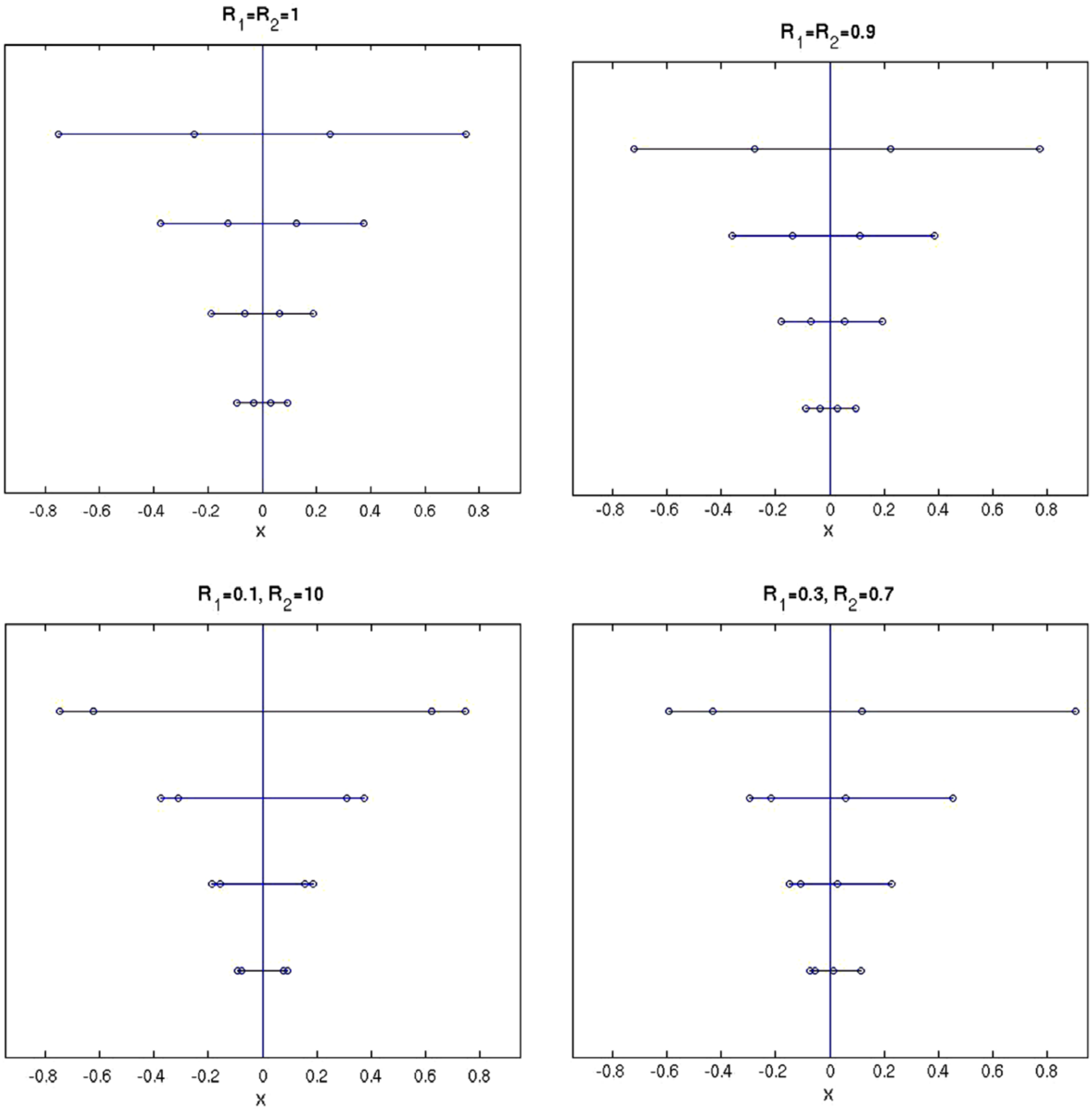

Fig. 4. Plots of the stencil points for the four test cases for the curvature error at the special point $\bar{x}^{(4)}_{5/2} = 0$ (the four-point average).

Table 1
Error in curvature at the special point $\bar{x}_{5/2}^{(4)} = 0$ (the four-point average of the stencil points). The meshes are shown in Fig. 4.

Width	Special point	Error	Order
1. $R_1 = R_2 = 1$			
h	0.0	1.87E−03	–
$h/2$	0.0	4.83E−04	1.95
$h/4$	0.0	1.22E−04	1.99
$h/8$	0.0	3.05E−05	2.00
2. $R_1 = R_2 = 0.9$			
h	0.0	1.92E−03	–
$h/2$	0.0	4.90E−04	1.97
$h/4$	0.0	1.23E−04	1.99
$h/8$	0.0	3.07E−05	2.00
3. $R_1 = 0.1, R_2 = 10$			
h	0.0	2.79E−03	–
$h/2$	0.0	7.33E−04	1.93
$h/4$	0.0	1.86E−04	1.98
$h/8$	0.0	4.65E−05	2.00
4. $R_1 = 0.3, R_2 = 0.7$			
h	0.0	2.34E−03	–
$h/2$	0.0	5.67E−04	2.04
$h/4$	0.0	1.38E−04	2.04
$h/8$	0.0	3.41E−05	2.02

Table 2
Error in first derivative at the left special point.

Width	Special point	Error	Order
1. $R_1 = R_2 = 1$			
h	−3.23E−01	9.78E−04	–
$h/2$	−3.23E−01	1.37E−04	2.87
$h/4$	−3.23E−01	1.79E−05	2.90
$h/8$	−3.23E−01	2.29E−06	2.97
2. $R_1 = R_2 = 0.9$			
h	−3.23E−01	8.80E−04	–
$h/2$	−3.23E−01	1.23E−04	2.84
$h/4$	−3.23E−01	1.62E−05	2.93
$h/8$	−3.23E−01	2.07E−06	2.97
3. $R_1 = 0.1, R_2 = 10$			
h	−3.99E−01	1.80E−03	–
$h/2$	−3.99E−01	2.64E−04	2.77
$h/4$	−3.99E−01	3.52E−05	2.91
$h/8$	−3.99E−01	4.53E−06	2.96
4. $R_1 = 0.3, R_2 = 0.7$			
h	−3.38E−01	5.62E−04	–
$h/2$	−3.38E−01	8.02E−05	2.81
$h/4$	−3.38E−01	1.06E−05	2.92
$h/8$	−3.38E−01	1.36E−06	2.96

To perform the convergence study, we mimic refining the mesh by dividing the stencil width h by two while keeping the same relative location of the four mesh points. This is illustrated in Fig. 4 for each test case, and all stencils illustrated there have the same mean point $\bar{x}_{5/2}^{(4)} = 0$.

The error E is calculated at a point that is fixed as the mesh refines,

$$E = |\phi - \phi_{exact}|, \tag{29}$$

where ϕ represent either the curvature

$$\kappa_{exact} = \frac{-y_{xx}}{(1 + y_x^2)^{3/2}} \tag{30}$$

at $\bar{x}_{5/2}^{(4)}$, or (later) the first derivative or the function at another appropriate fixed point.

Table 3
Error in function at the middle special point.

Width	Special point	Error	Order
1. $R_1 = R_2 = 1$			
h	0.0	5.52E−05	–
$h/2$	0.0	3.48E−06	3.99
$h/4$	0.0	2.18E−07	4.00
$h/8$	0.0	1.36E−08	4.00
2. $R_1 = R_2 = 0.9$			
h	−2.11E−02	5.51E−05	–
$h/2$	−2.11E−02	3.50E−06	3.98
$h/4$	−2.11E−02	2.20E−07	3.99
$h/8$	−2.11E−02	1.38E−08	4.00
3. $R_1 = 0.1, R_2 = 10$			
h	0.0	3.44E−04	–
$h/2$	0.0	2.17E−05	3.99
$h/4$	0.0	1.36E−06	4.00
$h/8$	0.0	8.50E−08	4.00
4. $R_1 = 0.3, R_2 = 0.7$			
h	−1.14E−01	5.98E−05	–
$h/2$	−1.14E−01	3.94E−06	3.92
$h/4$	−1.14E−01	2.52E−07	3.97
$h/8$	−1.14E−01	1.60E−08	3.98

Table 4
Error in curvature at a fixed point that is not the special point.

Width	Fixed point	Error	Order
1. $R_1 = R_2 = 1$			
h	−3.23E−01	8.66E−02	–
$h/2$	−3.23E−01	4.05E−02	1.10
$h/4$	−3.23E−01	1.94E−02	1.06
$h/8$	−3.23E−01	9.48E−03	1.03
2. $R_1 = R_2 = 0.9$			
h	−3.23E−01	8.66E−02	–
$h/2$	−3.23E−01	4.05E−02	1.10
$h/4$	−3.23E−01	1.94E−02	1.06
$h/8$	−3.23E−01	9.49E−03	1.03
3. $R_1 = 0.1, R_2 = 10$			
h	−3.99E−01	1.10E−01	–
$h/2$	−3.99E−01	5.06E−02	1.12
$h/4$	−3.99E−01	2.39E−02	1.08
$h/8$	−3.99E−01	1.17E−02	1.03
4. $R_1 = 0.3, R_2 = 0.7$			
h	−3.38E−01	9.10E−02	–
$h/2$	−3.38E−01	4.25E−02	1.10
$h/4$	−3.38E−01	2.03E−02	1.06
$h/8$	−3.38E−01	9.92E−03	1.03

The three mean values $\bar{f}_{i+1/2}$ (Eq. 4), i.e. the height functions $H_{i+1/2}$ (Eq. 1), are computed analytically by integrating Eq. (27) the cosine function. We use exact mean values to avoid the effect of such additional errors as those associated with numerical quadratures, or the inadequate choice of floors and ceilings. With these exact mean values, we compute the second and third difference quotients (Eqs. (6) and (7)), in order to compute the approximate curvature at the mean point $\bar{x}^{(4)}_{5/2}$ (the four-point average) by following the steps described in Section 2. The results of the error in curvature at that mean point are given in Table 1. These results show that the curvature is second-order accurate at the mean point $\bar{x}^{(4)}_{5/2}$ as expected.

The other two cases of testing convergence rates at a special point (relative to a stencil as it shrinks in size) are handled as follows. The special point is located at t^*, say, in the largest, h-size stencil interval. The stencil is then shrunk (say to width $h/2$) and then moved so that the location of the image of the special point in the shrunken stencil coincides with the location of t^* in the h-sized stencil. Now, the homogeneity associated with a scale change $t \leftarrow Ct$, applied to both t and the four t_i, is of degree 1, 2, and 3 in the linear, quadratic, and cubic cases, respectively. Consequently, the image of the special point in the

Table 5
Error in first derivative at a fixed point that is not a special point.

Width	Fixed point	Error	Order
1. $R_1 = R_2 = 1$			
h	0.0	2.16E−02	–
$h/2$	0.0	5.45E−03	1.99
$h/4$	0.0	1.36E−03	2.00
$h/8$	0.0	3.41E−04	2.00
2. $R_1 = R_2 = 0.9$			
h	0.0	2.17E−02	–
$h/2$	0.0	5.47E−03	1.99
$h/4$	0.0	1.37E−03	2.00
$h/8$	0.0	3.42E−04	2.00
3. $R_1 = 0.1, R_2 = 10$			
h	0.0	3.28E−02	–
$h/2$	0.0	8.30E−03	1.98
$h/4$	0.0	2.08E−03	2.00
$h/8$	0.0	5.21E−04	2.00
4. $R_1 = 0.3, R_2 = 0.7$			
h	0.0	2.41E−02	–
$h/2$	0.0	6.04E−04	2.00
$h/4$	0.0	1.51E−03	2.00
$h/8$	0.0	3.76E−04	2.01

Table 6
Error in function at a fixed point that is a special point for symmetric stencils (Cases 1 and 3) and that is not a special point for unsymmetric stencils (Cases 2 and 4).

Width	Fixed point	Error	Order
1. $R_1 = R_2 = 1$			
h	0.0	5.52E−05	–
$h/2$	0.0	3.48E−06	3.99
$h/4$	0.0	2.18E−07	4.00
$h/8$	0.0	1.36E−08	4.00
2. $R_1 = R_2 = 0.9$			
h	0.0	4.00E−04	–
$h/2$	0.0	5.39E−05	2.89
$h/4$	0.0	6.97E−06	2.95
$h/8$	0.0	8.85E−07	2.98
3. $R_1 = 0.1, R_2 = 10$			
h	0.0	3.44E−04	–
$h/2$	0.0	2.17E−05	3.99
$h/4$	0.0	1.36E−06	4.00
$h/8$	0.0	8.50E−08	4.00
4. $R_1 = 0.3, R_2 = 0.7$			
h	0.0	2.56E−03	–
$h/2$	0.0	3.26E−04	2.97
$h/4$	0.0	4.11E−05	2.99
$h/8$	0.0	5.15E−06	3.00

shrunken stencil is a special point with respect to the points in that smaller stencil. Moreover, it remains at the same *fixed* location with respect to the domain of the cosine function that comprises our test function.

We compute the approximate first derivative and approximate function at their special points, which are determined for the h-size stencil following the Remarks of Section 3 for $k = 3$. The approximate derivative is the linear function that interpolates the two successive second difference quotients $\Delta^2 F/\Delta t^2$. But, the approximate *function*, being the derivative of a cubic, is the quadratic function whose integral means are the three prescribed (integral) mean values $\bar{f}_{i+1/2}$. That is, the coefficients of the quadratic $c_3x^2 + c_2x + c_1$ are found by solving the following system of three equations for $m = i, i+1, i+2$:

$$\bar{f}_{m+1/2}(x_{m+1} - x_m) = c_3\frac{(x_{m+1}^3 - x_m^3)}{3} + c_2\frac{(x_{m+1}^2 - x_m^2)}{2} + c_1(x_{m+1} - x_m). \tag{31}$$

Table 7
Error in curvature, first derivative, and function at a fixed point ($x = 0.02$) that is not a special point.

Width	Curvature	Order	First derivative	Order	Function	Order
1. $R_1 = R_2 = 1$						
h	6.60E−03	–	2.16E−02	–	3.77E−04	–
$h/2$	2.85E−03	1.21	5.47E−03	1.98	5.13E−05	2.88
$h/4$	1.31E−03	1.13	1.37E−03	2.00	6.65E−06	2.95
$h/8$	6.23E−04	1.07	3.43E−04	2.00	8.46E−07	2.98
2. $R_1 = R_2 = 0.9$						
h	6.66E−03	–	2.17E−02	–	8.35E−04	–
$h/2$	2.86E−03	1.22	5.48E−03	1.99	1.09E−04	2.94
$h/4$	1.31E−03	1.13	1.37E−03	2.00	1.39E−05	2.97
$h/8$	6.23E−04	1.07	3.44E−04	2.00	1.75E−06	2.99
3. $R_1 = 0.1, R_2 = 10$						
h	7.54E−03	–	3.29E−02	–	3.14E−04	–
$h/2$	3.10E−03	1.28	8.34E−03	1.98	6.20E−05	2.34
$h/4$	1.37E−03	1.18	2.09E−03	1.99	9.14E−06	2.76
$h/8$	6.39E−04	1.10	5.24E−04	2.00	1.23E−06	2.90
4. $R_1 = 0.3, R_2 = 0.7$						
h	7.07E−03	–	2.42E−02	–	3.04E−03	–
$h/2$	2.93E−03	1.27	6.06E−03	2.00	3.88E−04	2.97
$h/4$	1.32E−03	1.15	1.51E−03	2.00	4.89E−05	2.99
$h/8$	6.27E−04	1.08	3.78E−04	2.00	6.13E−06	3.00

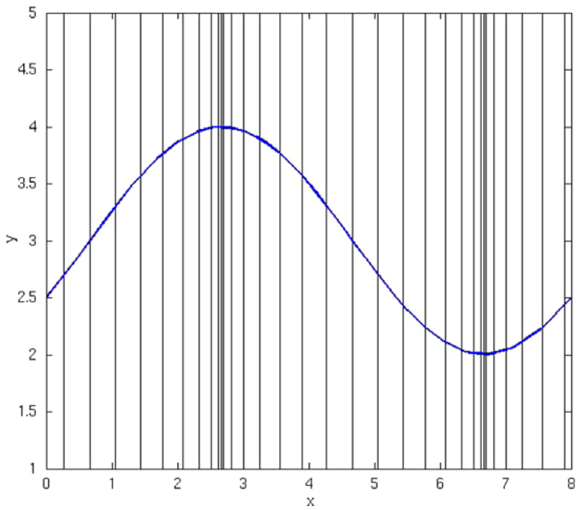

Fig. 5. Plot of the cosine function on a 32 point cosine-graded mesh.

The errors in the first derivative at one of the two special points are shown in Table 2, and the errors in the approximate function at the middle special point are shown in Table 3. As expected, the first derivative is third-order accurate at its special point, and the approximate function is fourth-order accurate at its special point. To check our calculations, we have estimated the curvature by differentiating the approximate quadratic function and found the results to match the ones obtained if curvature were computed using the difference quotients. This verification checks the coefficients of the quadratic function.

Finally, we estimate the curvature, first derivative and approximate function at a fixed point that is different from a special point, and investigate the errors at this fixed point. For curvature, we estimate the error at the fixed point that is the left special point for the first derivative, and for the first derivative and approximate function we use the curvature special point as the fixed point. The results are shown in Tables 4–6 for the curvature, first derivative and approximate function, respectively. As expected, at a fixed point that is different from their respective special points, the curvature is first-order accurate, the first derivative is second-order accurate and the approximate function is third-order accurate. Note that the fixed point for the approximate function for Cases 1 and 3 (the special point for curvature) is also the middle special point for the approximate function since those two stencils are symmetric. In Table 7, we show results for the error in curvature, first derivative and function at an arbitrary fixed point $x = 0.02$. Again, the curvature is found first-order accurate, the first

Table 8
Norms of curvature errors for the cosine function when the curvature is linearly interpolated from the four-point averages to the mesh points of uniform and cosine-graded meshes.

Number of points	L_1	Order	L_2	Order	L_∞	Order
Uniform mesh						
32	3.43E−03	–	4.84E−03	–	1.10E−02	–
64	8.41E−04	2.03	1.20E−03	2.01	2.83E−03	1.96
128	2.08E−04	2.02	2.97E−04	2.01	7.13E−04	1.99
256	5.19E−05	2.00	7.40E−05	2.00	1.79E−04	1.99
Cosine-graded mesh						
32	2.71E−03	–	3.00E−03	–	4.39E−03	–
64	7.39E−04	1.88	8.46E−04	1.82	1.31E−03	1.74
128	1.98E−04	1.90	2.22E−04	1.93	3.47E−04	1.92
256	5.05E−05	1.97	5.64E−05	1.98	8.79E−05	1.98

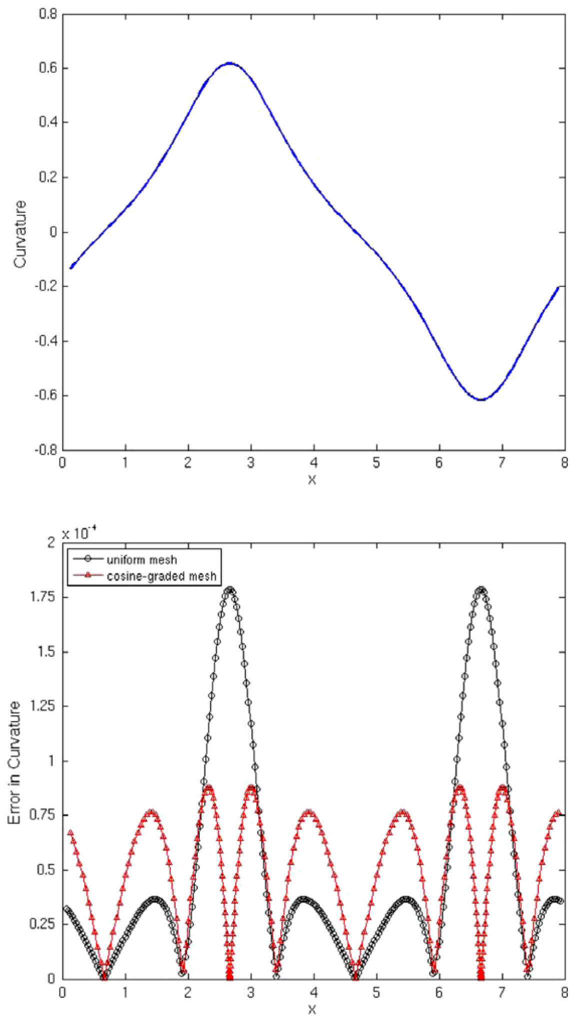

Fig. 6. Plots of the exact curvature and the error in curvature at the mesh points.

derivative second-order accurate and the approximate function third-order accurate. Note that as the mesh is shrunk (or the width is being divided by two), we translate the stencil to keep the fixed point stationary.

We now consider the cosine function (Eq. 27) on a cosine-graded mesh. The plot of the cosine function and the cosine-graded mesh of 32 points are shown in Fig. 5. We estimate the curvature at every mesh point by linearly interpolating the approximate curvature at the two neighboring special points (successive four-point averages) as described in Section 2 and perform a convergence study. The error norms are defined as:

Table 9
Error in curvature at the middle special point for a uniform stencil and a nonuniform stencil involving six successive points (five successive mean values). Initial width $h = 2.5$.

Width	Fixed point	Error	Order
Uniform mesh	$R_1 = R_2 = R_3 = R_4 = 1$		
h	0.0	9.43E−05	–
$h/2$	0.0	6.02E−06	3.97
$h/4$	0.0	3.78E−07	3.99
$h/8$	0.0	2.37E−08	4.00
Nonuniform mesh	$R_1 = 0.1, R_2 = 0.3, R_3 = 0.7, R_4 = 0.9$		
h	−0.1176	1.54E−04	–
$h/2$	−0.1176	8.78E−06	4.13
$h/4$	−0.1176	5.18E−07	4.08
$h/8$	−0.1176	3.13E−08	4.05

$$L_1 = \frac{\sum(|\kappa_i - \kappa_{exact}|\Delta x)}{\sum \Delta x}, \tag{32}$$

$$L_2 = \frac{\sqrt{\sum((\kappa_i - \kappa_{exact})^2 \Delta x)}}{\sum \Delta x}, \tag{33}$$

$$L_\infty = \max|\kappa_i - \kappa_{exact}|. \tag{34}$$

with $\Delta x = (x_{i+1} + x_i)/2 - (x_i + x_{i-1})/2$ for $i = 3, \ldots, N-2$ and where κ_i represents the interpolated curvature at the grid point x_i, κ_{exact} represents the exact curvature at the grid point x_i and N is the total number of mesh points.

The norms of curvature errors are shown in Table 8 for both uniform and cosine-graded meshes of 32, 64, 128 and 256 points. These results demonstrate that the interpolated curvature at grid points is second-order accurate, as expected. The curvature and the error in curvature for the 256-point uniform and cosine-graded meshes are plotted versus x in Fig. 6. Note that the cosine-graded mesh (which is finer at maximum curvature) reduces the maximum error in curvature.

Finally, Sussman and Ohta [14] recently estimated curvature to fourth-order accuracy using five adjacent columns of a uniform mesh instead of three. We now explain and demonstrate our extension of this to nonuniform rectangular grids.

More explicitly, $(x, f(x))$ is the unknown curve, F is an indefinite integral of f, we have five successive intervals bounded by six successive points

$$x_i < x_{i+1} < \cdots < x_{i+5}$$

and we take as given the five successive integral mean values $\bar{f}_{i+1/2} = (\Delta F/\Delta x)_{i+1/2}$ over these intervals. For curvatures, we need $d^2f/dx^2 = d^3F/dx^3$, which is approximated by the third derivative of the quintic polynomial interpolating the six successive mesh-point values of F. As such, that quadratic is $O(h^3)$ accurate over the whole interval $[x_i, x_{i+5}]$. But, we want fourth-order accuracy instead. That is associated naturally with the case $k = 5$ of the "Reworded Remark" in Section 3, and holds only at the three special points there. For curvatures at those points, one also needs fourth-order accurate approximations of $df/dx = d^2F/dx^2$ there. But that holds everywhere in $[x_i, x_{i+5}]$ using the first derivative of the quartic Q whose five mean values match the five mean values $\bar{f}_{i+1/2}, \ldots, \bar{f}_{i+9/2}$. (Alternatively, we could have evaluated the second-derivative of the Newton form of the quintic interpolating polynomial of the points $(x_i, F(x_i))_{i=0}^5$ with, say, $F(x_0) = 0$.)

The results for the error in curvature are shown in Table 9 for a uniform and a nonuniform mesh using five successive mean values. The curvature is found to be fourth-order accurate at the middle special point, as expected.

5. Conclusions

This note demonstrates both analytically and numerically that, respectively, curvatures can be computed to second-order accuracy, first derivatives to third-order accuracy, and curve locations to fourth-order accuracy, at special points associated locally with arbitrarily nonuniform rectangular grids, using three successive (integral) mean values (or "column" heights) as input data. Using five successive mean values instead, fourth-order accurate curvatures are similarly associated with three special points per six-point stencil. This note is an extension—and proof—of previous results obtained using the height function method to estimate curvatures when given volume fraction information on square grids.

Acknowledgments

The authors thank Rao Garimella and Sam Schofield for helpful discussions. The authors also thank one of the anonymous reviewers for the question: why not differentiate Cauchy's formula for the error in polynomial interpolation.

This work was performed under the auspices of the National Nuclear Security Administration of the US Department of Energy at Los Alamos National Laboratory under Contract No. DE-AC52-06NA25396 and supported by the Laboratory Directed Research and Development program 20070202ER.

Appendix A. Justification of the special accuracy at the special points

For $l = 0, 1, 2$ (and, indeed, up to $k-1$), respectively, we want to indicate why the $(k-l)$th derivative of the kth degree polynomial Pg (that interpolates the function g at the $k+1$ stencil points) has special accuracy $O(h^{2+l})$ at the $l+1$ special points of Section 3. (The ordinary accuracy, $O(h^{l+1})$, holds everywhere in the stencil interval $[t_0, t_k]$). So, let t^* be one of the special points. We modify the justification of the original Remark there, beginning just above Eq. (18). But, for the purposes of this Appendix, we assume that the origin $t = 0$ is placed at t^* (which is not necessarily $\bar{t}^{(k+1)}_{k/2}$ unless $l = 0$). We again involve the Maclaurin expansions M_k (Eq. 18) (about this new location) and the identity expressed in Eq. (19). Then, as $d^{k-l}(P(\cdot))/dt^{k-l}$ acts linearly, we conclude that (compare Eq. (20))

$$\frac{d^{k-l}(Pg)}{dt^{k-l}}(0) = \frac{d^{k-l}(PM_k g)}{dt^{k-l}}(0) + \left(\frac{d^{k+1}g}{dt^{k+1}}\right)(0) \cdot \frac{d^{k-l}\left(P\left[\frac{t^{k+1}}{(k+1)!}\right]\right)}{dt^{k-l}}(0) + \frac{d^{k-l}(PR_{k+1}g)}{dt^{k-l}}(0). \tag{A.1}$$

Since $P(M_k) = M_k$, the first term on the right of Eq. (A.1) is $(d^{k-l}g/dt^{k-l})(0)$. The special point $t^*(=0)$ is either $\bar{t}^{(k+1)}_{k/2}$ (when $l = 0$) or one of the other special points at the end of the Reworded Remark in Section 3. So, the second factor of the second term in Eq. (A.1) is zero. Thus,

$$\frac{d^{k-l}(Pg)}{dt^{k-l}}(t^*) = \left(\frac{d^{k-l}g}{dt^{k-l}}\right)(t^*) + \frac{d^{k+1}g}{dt^{k+1}}(0) \cdot 0 + \frac{d^{k-l}(PR_{k+1}g)}{dt^{k-l}}(t^*). \tag{A.2}$$

Since $R_{k+1}g$ is $O(h^{k+2})$, the last term is $O(h^{k+2-(k-l)}) = O(h^{2+l})$. Thus, the Reworded Remark is justified.

References

[1] S. Afkhami, M. Bussmann, Height functions for applying contact angles to 2D VOF simulations, International Journal for Numerical Methods in Fluids 57 (2008) 453–472.
[2] R.S. Burington, Handbook of Mathematical Tables and Formulas, third ed., Handbook Publishers, Sandusky, Ohio, 1953.
[3] S.J. Cummins, M.M. Francois, D.B. Kothe, Estimating curvature from volume fractions, Computers and Structures 83 (2005) 425–434.
[4] P.A. Ferdowsi, M. Bussmann, Second-order accurate normals from height functions, Journal of Computational Physics 227 (2008) 9293–9302.
[5] M.M. Francois, S.J. Cummins, E.D. Dendy, D.B. Kothe, J.M. Sicilian, M.W. Williams, A balanced-force algorithm for continuous and sharp interfacial surface tension models within a volume tracking framework, Journal of Computational Physics 213 (2006) 141–173.
[6] W. Gautschi, Numerical Analysis: An Introduction, Birkhauser, Boston, 1997.
[7] J. Helmsen, P. Colella, E.G. Puckett, Non-convex profile evolution in two dimensions using volume of fluids, LBNL Technical Report LBNL-40693, Lawrence Berkeley National Laboratory, 1997.
[8] J. Hernandez, J. Lopez, P. Gomez, C. Zanzi, F. Faura, A new volume of fluid method in three dimensions – Part I: Multidimensional advection method with face-matched flux polyhedra, International Journal for Numerical Methods in Fluids 58 (2008) 897–921.
[9] H.-O. Kreiss, T. Manteuffel, B. Swartz, B. Wendroff, A. White, Supra-convergent schemes on irregular grids, Mathematics of Computation 47 (1986) 537–554.
[10] D. Lorstad, M.M. Francois, W. Shyy, L. Fuchs, Assessment of volume of fluid and immersed boundary methods for droplet computations, International Journal for Numerical Methods in Fluids 46 (2004) 109–125.
[11] R. Mjolsness, B. Swartz, Some plane curvature approximations, Mathematics of Computation 49 (1987) 215–230.
[12] S. Popinet, An accurate adaptive solver for surface-tension-driven interfacial flows, Journal of Computational Physics 228 (2009) 5838–5866.
[13] M. Sussman, A second order coupled level set and volume-of-fluid method for computing growth and collapse of vapor bubbles, Journal of Computational Physics 187 (2003) 110–136.
[14] M. Sussman, M. Ohta, High-order techniques for calculating surface tension forces, International Series of Numerical Mathematics 154 (2007) 425–434.
[15] M.D. Torrey, L.D. Cloutman, R.C. Mjolsness, C.W. Hirt, NASA-VOF2D: a computer program for incompressible flows with free surfaces, LANL Technical Report LA-10612-MS, Los Alamos National Laboratory, 1985.
[16] A.E.P. Veldman, J. Gerrits, R. Luppes, J.A. Helder, J.P.B. Vreeburg, The numerical simulation of liquid sloshing on board spacecraft, Journal of Computational Physics 224 (2007) 82–99.
[17] <http://mathworld.wolfram.com>.